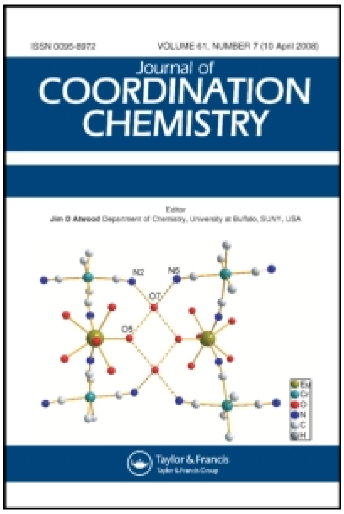

Journal of Coordination Chemistry
Publication details, including instructions for authors and subscription information:
http://www.informaworld.com/smpp/title~content=t713455674

Supramolecular networks constructed by cationic copper(II) complexes incorporating hybrid water-anionic polymeric assemblies

Xia Li[a]; Xiao Qiu[a]
[a] Department of Chemistry, Capital Normal University, Beijing 100048, People's Republic of China

To cite this Article Li, Xia and Qiu, Xiao(2010) 'Supramolecular networks constructed by cationic copper(II) complexes incorporating hybrid water-anionic polymeric assemblies', Journal of Coordination Chemistry, 63: 23, 4077 — 4087
To link to this Article: DOI: 10.1080/00958972.2010.531713
URL: http://dx.doi.org/10.1080/00958972.2010.531713

Journal of Coordination Chemistry
Vol. 63, No. 23, 10 December 2010, 4077–4087

Supramolecular networks constructed by cationic copper(II) complexes incorporating hybrid water–anionic polymeric assemblies

XIA LI* and XIAO QIU

Department of Chemistry, Capital Normal University, Beijing 100048,
People's Republic of China

(*Received 10 May 2010; in final form 22 September 2010*)

Two complexes, $[Cu_2(TFSA)(2,2'\text{-bpy})_4]\cdot TFSA\cdot 8H_2O$ (**1**) and $\{[Cu(4,4'\text{-bpy})(H_2O)_2]\cdot TFSA\cdot 6H_2O\}_n$ (**2**) (H_2TFSA = tetrafluorosuccinic acid, 2,2′-bpy = 2,2′-bipyridine, and 4,4′-bpy = 4,4′-bipyridine), have been synthesized and structurally characterized by X-ray structural analyses. Complex **1** is a binuclear molecule bridged by TFSA ligands; **2** is a 1-D chain bridged by 4,4′-bpy ligands. The asymmetric units of the two complexes are composed of cationic complexes $[Cu_2(TFSA)(2,2'\text{-bpy})_4]^{2+}$ (**1**) and $[Cu(4,4'\text{-bpy})(H_2O)_2]^{2+}$ (**2**), free TFSA anion, and independent crystallization water molecules. A unique 2-D hybrid water–TFSA anionic layer by linkage of $\{[(H_2O)_8(TFSA)]^{2-}\}_n$ fragments consisting of 1-D T6(0)A2 water tape and TFSA anionic units by hydrogen bonds in **1** was observed. Unique 2-D hybrid water–TFSA anionic layer generated by the linkage of $\{[(H_2O)_6(TFSA)]^{2-}\}_n$ fragments consisting of cyclic water tetramers with appended water molecules and TFSA anionic units, and 1-D metal–water tape $[Cu–H_2O\cdots(H_2O)_6\cdots H_2O^-]_n$ in **2** were found. 3-D supramolecular networks of the two complexes consist of cationic complexes and water–TFSA anionic assemblies connected by hydrogen bonds.

Keywords: Copper complex; Tetrafluorosuccinic acid; Hybrid water-anion assembly; Supramolecular network

1. Introduction

Metal–organic frameworks (MOFs) have been studied due to their diverse structural motifs and applications in catalysis, magnetism, fluorescent materials, etc. [1–8]. Construction of MOFs generally utilizes multifunctional organic molecules as linkage through metal–ligand covalent bonds [1–15]. Low-dimensional metal complexes as building blocks to assemble higher-dimensional supramolecular networks have also been reported [16–39]. The use of noncovalent interactions such as hydrogen bonds and π–π stacking interactions is useful for the design of supramolecular networks from molecular building blocks. Interest has been focused on supramolecular networks constructed from hydrogen bonds. Solvent molecules, especially free water in the crystals,

---

*Corresponding author. Email: xiali@mail.cnu.edu.cn

Journal of Coordination Chemistry
ISSN 0095-8972 print/ISSN 1029-0389 online © 2010 Taylor & Francis
DOI: 10.1080/00958972.2010.531713

often affect self-assembly of crystal structures through hydrogen bonds and can stabilize supramolecular species. Water clusters have been intensively investigated both theoretically and experimentally due to their importance in biological and chemical processes [40, 41]. A number of discrete water clusters with different configurations have been reported in supramolecular hosts [16–27]. Infinite chain, tape, and layer water arrays based on cyclic water units have been assembled [28–35]. Relatively less attention has focused on hybrid water assemblies with other solvents, small molecules, or counterions by hydrogen bonds [42, 43]. These hydrogen bonds in crystals lead to supramolecular networks.

Carboxylates can bridge metal centers to produce intriguing architectures *via* covalent bonds and/or hydrogen bonds. In a previous work, we demonstrated that tetrafluorosuccinic acid (H_2TFSA) is a bridge for the formation of lanthanide–MOFs [44, 45]. This study is an extension of the above studies with two new complexes $[Cu_2(TFSA)(2,2'\text{-bpy})_4] \cdot TFSA \cdot 8H_2O$ (**1**) and $\{[Cu(4,4'\text{-bpy})(H_2O)_2] \cdot TFSA \cdot 6H_2O\}_n$ (**2**) (H_2TFSA = tetrafluorosuccinic acid, 2,2′-bpy = 2,2′-bipyridine, and 4,4′-bpy = 4,4′-bipyridine) obtained by reactions of Cu^{2+} and characterized by single-crystal X-ray diffractometry. Complex **1** is a discrete binuclear molecule and **2** is a polymeric chain. The asymmetric units of the two complexes are composed of a Cu^{2+}-complex cation, free anions, and crystallization water molecules. Novel water morphologies in the two complexes are observed. This study presents the synthesis and structural characterization of the two complexes, emphasizing the water clusters, water tape, and the unique hybrid water–anionic assemblies.

2. Experimental

2.1. *Synthesis of the complexes*

2.1.1. $[Cu_2(TFSA)(2,2'\text{-bpy})_4] \cdot TFSA \cdot 8H_2O$ (1). A mixture of $CuSO_4$ (0.0320 g, 0.2 mmol), tetrafluorosuccinic acid (0.0380 g, 0.2 mmol), 2, 2′-bipyridine (0.0312 g, 0.2 mmol), sodium hydroxide aqueous solution (2.0 mol L^{-1}, 0.20 mL), and deionized water (8 mL) in a 25 mL Teflon-lined stainless steel autoclave was heated under autogenous pressure at 150°C for 3 days, and then cooled to room temperature at a rate of 10°C h^{-1}. The resulting solution was filtered and light blue block single crystals were obtained (the crystals formed during the cooling process). Yield: 57% (based on Cu). Anal. Calcd (Found) for $C_{24}H_{22}F_4N_4O_8Cu$ (%): C, 45.43 (45.12); H, 3.50 (3.76); N, 8.84 (8.67). Selected IR (KBr pellet; ν, cm^{-1}): 3431 s, 1674 s, 1600 m, 1495 w, 1475 w, 1446 m, 1371 m, 1383 w, 1136 m, 1105 m, 773 m, 732 w, and 422 w.

2.1.2. $\{[Cu(4,4'\text{-bpy})(H_2O)_2] \cdot TFSA \cdot 6H_2O\}_n$ (2). The synthetic procedure of **2** was similar to that of **1** except 2,2′-bipyridine was replaced by 4,4′-bipyridine (0.0312 g, 0.2 mmol). The resulting solution was filtered and light blue block single crystals were obtained from the mother liquid after several weeks. Yield: 55% (based on Cu). Anal. Calcd (Found) for $C_{14}H_{24}F_4N_2O_{12}Cu$ (%): C, 30.47 (30.22); H, 4.38 (4.55); and N, 5.07 (5.21). Selected IR (KBr pellet; ν, cm^{-1}): 3423 s, 1678 s, 1613 s, 1494 w, 1420 m, 1382 s, 1136 s, 814 m, 730 w, 496 w, and 414 w.

2.2. *Materials and physical measurements*

All chemicals used for synthesis are of analytical grade and commercially available. Elemental analyses (C, H, and N) were performed using an Elementar Vario EL analyzer. IR spectra (4000–400 cm^{-1}) were recorded on a Bruker EQUINOX-55 using KBr pellets. Thermogravimetric analyses (TGA) were carried out on a WCT-1A Thermal Analyzer at a heating rate of $10^{\circ}\mathrm{C\,min}^{-1}$ from room temperature to 1000°C in air.

2.3. *X-ray crystal structure determination*

Single crystals for **1** and **2** were selected for structural analysis. Data collections were performed at 296(2) K on a Bruker Smart Apex II CCD diffractometer with graphite-monochromated Mo-Kα radiation ($\lambda = 0.71073$ Å). Semi-empirical absorption corrections were applied using SADABS. The structure was solved by direct methods and refined by full-matrix least-squares on F^2 using SHELXS-97 and SHELXL-97, respectively [46, 47]. Summary of the crystallographic data and details of the structure refinements are listed in table 1. Selected bond lengths and angles of **1** and **2** are listed in tables 2 and 3, respectively.

Table 1. Crystallographic data and refinement details for **1** and **2**.

	1	**2**
Empirical formula	$C_{24}H_{22}F_4N_4O_8Cu$	$C_{14}H_{24}F_4N_2O_{12}Cu$
Formula weight	634.00	551.90
Crystal system	Triclinic	Monoclinic
Space group	$P\bar{1}$	$C2/c$
Unit cell dimensions (Å, °)		
a	12.1833(5)	17.0833(3)
b	14.7443(6)	11.1127(2)
c	15.7153(7)	12.1044(2)
α	90.089(2)	90
β	107.904(2)	104.8570(10)
γ	93.027(2)	90
Volume (Å^3), Z	882.84(15), 4	2221.10(7), 4
Calculated density ($\mathrm{Mg\,m}^{-3}$)	1.570	1.650
Absorption coefficient (mm^{-1})	0.897	1.079
$F(000)$	1292	1132
Crystal size (mm^3)	0.20 × 0.12 × 0.10	0.30 × 0.15 × 0.10
θ range for data collection (°)	2.36–25.01	2.21–27.90
Limiting indices	$-14 \le h \le 14$; $-17 \le k \le 17$; $-18 \le l \le 17$	$-21 \le h \le 22$; $-14 \le k \le 14$; $-15 \le l \le 15$
Reflections collected	29,863	16,948
Independent reflection	9206 [R(int) = 0.0425]	2646 [R(int) = 0.0210]
Data/restraints/parameters	9206/0/748	2646/0/153
Goodness-of-fit on F^2	1.021	1.053
Final R indices [$I > 2\sigma(I)$]	$R_1 = 0.0599$, $wR_2 = 0.1564$	$R_1 = 0.0245$, $wR_2 = 0.0707$
R indices (all data)	$R_1 = 0.0817$, $wR_2 = 0.1696$	$R_1 = 0.0266$, $wR_2 = 0.0722$
Largest difference peak and hole (e Å^{-3})	0.862 and −0.547	0.406 and −0.352
CCDC	730733	730735

Table 2. Selected bond lengths (Å) and angles (°) of **1**.

Cu(1)–N(1)	2.083(4)	Cu(1)–N(2)	1.981(4)
Cu(1)–N(3)	2.057(4)	Cu(1)–N(4)	1.974(4)
Cu(1)–O(1)	2.069(3)	Cu(2)–O(4)	2.039(3)
Cu(2)–N(5)	2.048(4)	Cu(2)–N(6)	1.972(4)
Cu(2)–N(7)	1.976(4)	Cu(2)–N(8)	2.084(4)
O(1)–Cu(1)–N(1)	111.43(14)	O(1)–Cu(1)–N(2)	87.34(15)
O(1)–Cu(1)–N(3)	124.65(14)	O(1)–Cu(1)–N(4)	90.87(15)
N(1)–Cu(1)–N(2)	80.10(15)	N(1)–Cu(1)–N(3)	123.91(16)
N(1)–Cu(1)–N(4)	100.27(15)	N(2)–Cu(1)–N(3)	100.24(15)
N(2)–Cu(1)–N(4)	178.18(17)	N(3)–Cu(1)–N(4)	81.07(15)
O(4)–Cu(2)–N(5)	128.38(15)	O(4)–Cu(2)–N(6)	91.05(15)
O(4)–Cu(2)–N(7)	88.01(15)	O(4)–Cu(2)–N(8)	112.26(14)
N(5)–Cu(2)–N(6)	81.03(16)	N(5)–Cu(2)–N(7)	100.52(16)
N(5)–Cu(2)–N(8)	119.37(15)	N(6)–Cu(2)–N(7)	178.45(16)
N(6)–Cu(2)–N(8)	99.00(15)	N(7)–Cu(2)–N(8)	80.22(15)

Table 3. Selected bond lengths (Å) and angles (°) of **2**.

Cu(1)–O(4W)	1.9743(10)	Cu(1)–O(4W)^a	1.9743(10)
Cu(1)–N(1)	2.0131(15)	Cu(1)–N(2)^b	2.0215(16)
O(4W)–Cu(1)–O(4W)^a	178.14(5)	O(4W)–Cu(1)–N(1)	89.07(3)
O(4W)–Cu(1)–N(2)^b	90.93(3)	O(4W)^a–Cu(1)–N(1)	89.07(3)
O(4W)^a–Cu(1)–N(2)^b	90.93(3)	N(1)–Cu(1)–N(2)^b	180.0

Symmetry transformations used to generate equivalent atoms: $^a[-x, y, -z+1/2]$; and $^b[x, y+1, z]$.

3. Results and discussion

3.1. *Crystal structure of [Cu_2(TFSA)(2,2′-bpy)$_4$]•TFSA•$8H_2O$ (1)*

IR spectra of **1** exhibit absorption bands, $\nu_{as(COO)}$ at 1600 cm^{-1} and $\nu_{s(COO)}$ at 1371 cm^{-1}. The $\Delta(\nu_{as}-\nu_s)$ value is 229 cm^{-1}, showing that carboxylate is monodentate, consistent with the result of X-ray structure analysis.

The structure of [Cu_2(TFSA)(2,2′-bpy)$_4$]·TFSA·$8H_2O$ (**1**), shown in figure 1, consists of [Cu_2(TFSA)(2,2′-bpy)$_4$]$^{2+}$–{Cu_2}$^{2+}$, a free TFSA anion, and eight lattice water molecules (figure 1a). The coordination geometries of Cu(1) and Cu(2) are similar. The two Cu^{2+} are bridged by a single TFSA forming a dimer with Cu···Cu distance of 8.970(7) Å. TFSA coordinates Cu^{2+} by the rare bis(monodentate). The two chelating 2,2′-bpy molecules coordinate Cu^{2+} ion with a twist angle of 50.4°. Cu^{2+} is five coordinate in a distorted trigonal bipyramid, in which N2 and N4 occupy axial positions [*d*(Cu1–N) = 1.981(4) and 1.974(4) Å], while the equatorial positions are furnished by N1, N3, and O1 [*d*(Cu1–N) = 2.083(4) Å and 2.057(4) Å, *d*(Cu1–O) = 2.069(3) Å]. The equatorial Cu–N bond lengths are slightly longer than the corresponding axial Cu–N bond lengths. The N2–Cu1–N4 bond angle of 178.18(17)° is slightly distorted from 180°. The 2,2′-bpy molecules form hydrogen bonds with TFSA ligands from adjacent coordination cations. C–H···F and C–H···O hydrogen bonds with C···F and C···O distances range from 3.214(7) to 3.317(6) Å and 3.123(7) to 3.530(6) Å, respectively (table 4). C–H···F interactions are comparable to those found in other reported complexes [48–54]. Moreover, the H···F distances

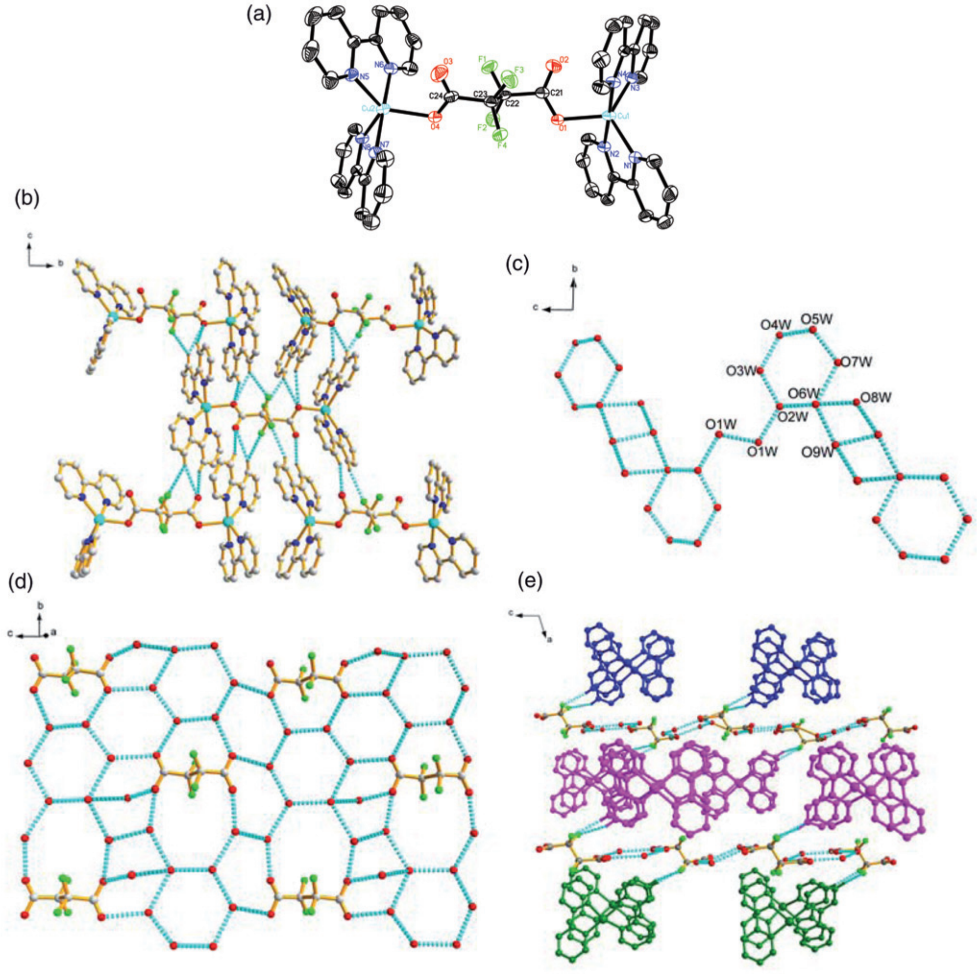

Figure 1. View of the structure of **1**: (a) Molecular structure at the 30% probability displacement ellipsoids. All hydrogens, uncoordinated water molecules and TFSA are omitted for clarity. (b) 2-D cationic layer based on $[Cu_2(TFSA)(2,2'\text{-bpy})_4]^{2+}$ by C–H ··· F and C–H ··· O hydrogen bonds. (c) 1-D water tape with the symbol of T6(0)A2. (d) 2-D hybrid water–TFSA anionic layer. (e) 3-D supramolecular structure consisting of 2-D cationic layers and 2-D anionic layers by hydrogen bonds.

vary from 2.50 to 2.58 Å within the sum of van der Waal's radii of fluorine and hydrogen (2.67 Å). Thus, $[Cu_2(TFSA)(2,2'\text{-bpy})_4]^{2+}$ build up a 2-D cationic layer by C–H ··· F and C–H ··· O hydrogen bonds (figure 1b).

In the crystal structure of **1**, all the lattice water molecules and free TFSA are involved in hydrogen bonds to form a unique 2-D hybrid water–TFSA anionic layer. Hydrogen bonding parameters for **1** are listed in table 4. There are eight lattice water molecules and the disordered lattice water molecules O8W and O9W have split occupancy of 0.50. All crystal water molecules in the asymmetric unit are involved in forming a $(H_2O)_8$ cluster by strong O–H ··· O hydrogen bonds; O2W ··· O3W ··· O4W ··· O5W ··· O7W ··· O6W affords a cyclic centrosymmetric

Table 4. Hydrogen bonding parameters for **1**.

D–H···A	D–H	H···A	D···A	D–H···A
O2W–H2WB···O6W	0.90	2.05	2.811(9)	141
O3W–H3WB···O2W	0.93	1.94	2.771(8)	148
O4W–H4WB···O3W	0.90	2.04	2.741(8)	133
O7W–H7WB···O5W^{a}	0.89	1.86	2.705(1)	158
O6W–H6WA···O7W^{b}	0.87	2.59	3.038(1)	120
O2W–H2WA···O1W^{c}	0.90	1.95	2.833(7)	165
O6W–H6WB···O9W	0.91	2.22	3.022(2)	147
O7W–H7WA···O8W	0.91	2.27	3.085(2)	150
O1W–H1WA···O8^{a}	0.88	1.91	2.731(7)	156
O4W–H4WA···O7^{d}	0.88	1.94	2.791(7)	164
C4–H4A···F2^{e}	0.93	2.50	3.214(7)	134
C8–H8A···F6^{f}	0.93	2.51	3.118(7)	123
C26–H26A···F7^{g}	0.93	2.53	3.193(1)	128
C31–H31A···F1^{i}	0.93	2.56	3.317(6)	139
C32–H32A···F7^{j}	0.93	2.56	3.375(9)	147
C41–H41A···F4^{c}	0.93	2.58	3.215(6)	126
C4–H4A···O4^{g}	0.93	2.69	3.530(6)	151
C7–H7A···O1^{g}	0.93	2.62	3.477(6)	153
C17–H17A···O2^{g}	0.93	2.23	3.123(7)	161
C28–H28A···O3^{d}	0.93	2.44	3.237(8)	143

Symmetry transformations used to generate equivalent atoms: $^{a}[x+1, y, z]$; $^{b}[x-1, y-1, z]$; $^{c}[-x+1, -y, -z]$; $^{d}[-x+1, -y+1, -z]$; $^{e}[x-1, y, z-1]$; $^{f}[-x+1, -y+1, -z+1]$; $^{g}[-x+1, -y, -z+1]$; $^{i}[-x+1, -y, -z+1]$; $^{j}[x, y-1, z]$.

water cluster $(H_2O)_6$ that adopts hexagonal ice-like conformation. The O···O distances in the hydrogen bonds range from 2.705(1) to 3.085(2) Å, with an average value of 2.802 Å, shorter than 2.854 Å in liquid water and longer than 2.759 Å in ice I_h [55, 56]. The bond angles of O1W–O2W–O3W, O2W–O3W–O1WA, and O3W–O1WA–O2WA are 120.77°, 118.78°, and 104.45°, respectively. The hexameric water cluster is particularly interesting because this cluster can exhibit some properties of bulk water and may provide an interesting model for the smallest piece of ice [57]. The hexamer $(H_2O)_6$ is further connected to the remaining two lattice water molecules (O1W and O9W) to form an octameric water cluster $(H_2O)_8$ through O–H···O interactions with O1W···O2W distance of 2.833(7) Å and O6W···O9W distance of 3.022(2) Å. These water clusters are extended through water–water interactions to give a unique 1-D water tape with symbol of T6(0)A2 [28] (figure 1c). Furthermore, water octamers form hydrogen bonds with free TFSA through O–H···O interactions with O1W···O8 distance of 2.731(7) Å and O4W···O7 distance of 2.791(7) Å, leading to formation of a 2-D hybrid water–TFSA anionic layer by linkage of $\{[(H_2O)_8(TFSA)]^{2-}\}_n$ fragments (figure 1d).

The crystal structure of **1** consists of two parts. One is a 2-D cationic layer of $[Cu_2(TFSA)(2,2'\text{-bpy})_4]^{2+}$ constructed by C–H···F and C–H···O hydrogen bonds. The other is the 2-D anionic layer of lattice water molecules and TFSA by hydrogen bonds. Both layers are connected by hydrogen bonds (table 4) and arrayed alternately to form a 3-D network structure (figure 1e). Complex **1** can be considered as an unusual set of water–TFSA anionic "hosts" with cationic $\{Cu_2\}^{2+}$ "guests." Moreover, this study extends the limited number of examples of polymeric 2-D hybrid water–anionic assemblies intercalated in crystalline materials.

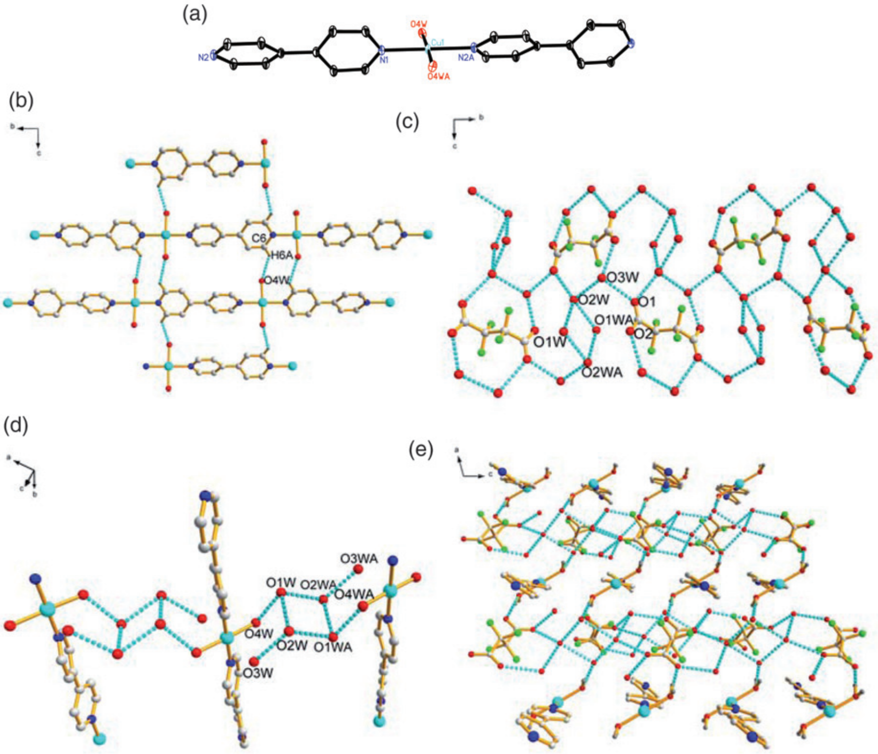

Figure 2. View of the structure of **2**: (a) Molecular structure at the 30% probability displacement ellipsoids. All hydrogens, uncoordinated water and TFSA are omitted for clarity. (b) 2-D cationic layer based on the 1-D $\{[Cu(4,4'\text{-bpy})(H_2O)_2]\}_n^{2+}$ by C–H $\cdots$ O hydrogen bonds. (c) 2-D hybrid water–TFSA anionic layer consisting of cyclic water tetramers with appended water and TFSA anionic units. (d) 1-D metal–water tape. (e) Packing diagram showing the 3-D supramolecular structure by hydrogen bonds.

3.2. *Crystal structure of* $\{[Cu(4,4'\text{-bpy})(H_2O)_2]\cdot TFSA\cdot 6H_2O\}_n$ *(2)*

Complex **2** consists of a 1-D chain, as shown in figure 2. Within the structure, Cu^{2+} are bridged by 4,4′-bpy into a cationic chain $\{[Cu(4,4'\text{-bpy})(H_2O)_2]\}_n^{2+}-\{Cu\}_n^{2+}$. All Cu^{2+} are linear with Cu $\cdots$ Cu separation of 6.665(5) Å. Pyridyl rings of 4,4′-bpy are not coplanar with a dihedral angle of 23.9°. The asymmetric unit of **2** contains $[Cu(4,4'\text{-bpy})(H_2O)_2]^{2+}$, free TFSA anion, and water (figure 2a). Cu^{2+} is coordinated by two nitrogens of two 4,4′-bpy ligands [d(Cu1–N) = 2.0131(15) and 2.0215(16) Å] and two water molecules [d(Cu1–OW) = 1.9740 Å]. The CuN_2O_2 lies exactly in the same plane with Cu^{2+} a slightly distorted square with the angles O4W–Cu1–N1 and O4W–Cu1–N2A of 89.07(3)° and 90.93(3)°, respectively. Hydrogen bonds form between adjacent 1-D chains from 4,4′-bpy and coordinated water; C6–H6A $\cdots$ O4W hydrogen bonds with C $\cdots$ O distance of 3.320(2) Å give a 2-D cationic layer (figure 2b).

The most striking feature of the crystal structure of **2** is lattice $(H_2O)_6$ clusters, unique 2-D hybrid water–TFSA anionic layer, and metal–octamer water chains by hydrogen bonds, forming a 3-D supramolecular network. Hydrogen bonding parameters for **2** are listed in table 5. Lattice water molecules O1W and O2W are connected with two

Table 5. Hydrogen bonding parameters for **2**.

D–H···A	D–H	H···A	D···A	D–H···A
O2W–H2WB···O1	0.98	1.89	2.869(2)	172
O1W–H1WA···O2W[a]	0.89	1.95	2.824(2)	166
O1W–H1WB···O2W	0.89	2.02	2.871(2)	158
O2W–H2WA···O3W	0.89	1.93	2.819(2)	174
O3W–H3WA···O2	0.89	1.93	2.815(2)	173
O4W–H4WB···O1W[b]	0.89	1.80	2.690(2)	175
O3W–H3WB···O1[c]	0.90	1.82	2.719(2)	177
C1–H1A···F2	0.93	2.37	3.230(2)	154
C6–H6A···O4W[d]	0.93	2.58	3.320(2)	137

Symmetry transformations used to generate equivalent atoms: [a][-0.5, $-y-0.5$, $z+0.5$]; [b][$-x$, y, $0.5-z$]; [c][$0.5-x$, $0.5+y$, $0.5-z$]; and [d][x, $-y$, $z+0.5$].

centrosymmetrically related water molecules (O1WA and O2WA) by two-fold O1W···O2W and O1W···O2WA hydrogen bonds, forming a cyclic planar tetrameric water cluster with symbol of R4 [22] (figure 2c). A two-fold symmetry axis perpendicular to the O1W···O2W···O1WA···O2WA plane is observed, suggesting that the tetrameric water cluster has C_{2h} symmetry [27]. In the tetrameric water cluster, O2W is a double hydrogen bond acceptor and O1W a double hydrogen bond donor. Two lattice water molecules O3W and O3WA are appended to the upper and lower sides of the tetrameric water motif *via* O2W···O3W and O2WA···O3WA hydrogen bonds, forming a discrete lattice water hexamer $(H_2O)_6$ with O···O distances ranging from 2.819(2) to 2.871(2) Å. The discrete $(H_2O)_6$ clusters and free TFSA form a unique 2-D hybrid water–TFSA anionic layer generated by linkage of $\{[(H_2O)_6(TFSA)]^{2-}\}_n$ fragments through O2W···O1 and O3W···O2 hydrogen bonds with O···O distances of 2.869(2) and 2.815(2) Å, respectively (figure 2c). The $(H_2O)_6$ clusters form discrete water octamers with O4W and O4WA binding to the metal ion by O1W···O4W and O1WA···O4WA hydrogen bonds with O···O distance of 2.690(2) Å. This water octamer assumes a chair conformation, in which the O3W and O4W are located at the upper and lower sides of the planar four-membered ring. The O4W–O1W–O2W or O3W–O2W–O1W angles are 96.62° and 93.58°, respectively. The water octamers link Cu^{2+} ions of adjacent 1-D coordination chains $[\text{–Cu–(4,4'-bpy)–}]_n$ to form a rare 1-D metal–water tape by linkage of $[Cu\text{–}H_2O\cdots(H_2O)_6\cdots H_2O]_n$ fragments (figure 2d). The 1-D metal–water tape $[Cu\text{–}H_2O\cdots(H_2O)_6\cdots H_2O]_n$ and 1-D $[\text{–Cu–(4,4'-bpy)–}]_n$ polymeric chain are along two different directions. In addition, the C–H···F interactions with C···F distance of 3.230(2) Å form between hydrogen of 4,4′-bpy molecules and the fluorines of uncoordinated TFSA [48–54]. Interactions of the hybrid water–TFSA anionic layer and metal–water tapes result in a 3-D supramolecular network (figure 2e). The 3-D supramolecular network of **2** is made up of alternating layers of 2-D cationic and 2-D anionic layers linked by O1W···O4W and C–H···F hydrogen bonds.

3.3. *Thermogravimetric analysis*

DTA–TGA analyses of the two complexes were performed between room temperature and 1000°C (figures 3 and 4). The first weight loss occurs between 86–138°C for **1** and 83–237°C for **2**, caused by loss of all water molecules. The weight losses are 11.42% (calculated, 11.40%) for **1** and 26.19% (calculated, 26.11%) for **2**. The organic ligands

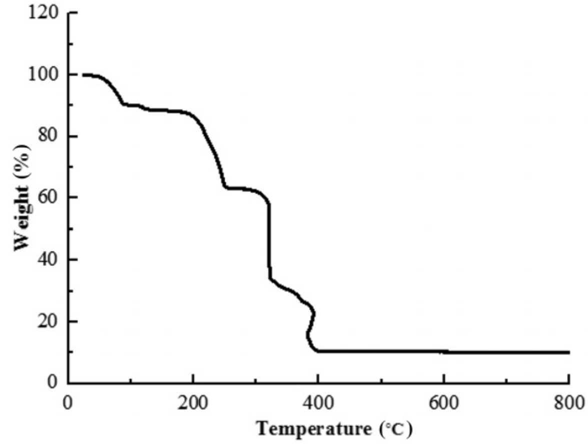

Figure 3. TGA curve of **1**.

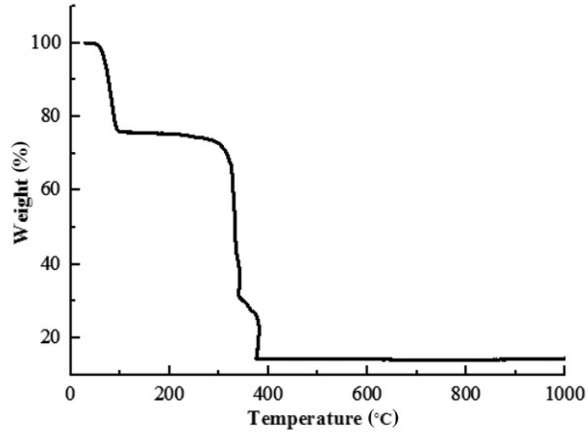

Figure 4. TGA curve of **2**.

completely decomposed at 385°C for **1** and 382°C for **2**, respectively. The total weight losses of 89.44% for **1** and 85.71% for **2** suggest decomposition leaving CuO as the final products, which is corroborated by the calculated values of 87.41% for **1** and 85.59% for **2**.

4. Conclusion

Synthesis and crystal structures of $[Cu_2(TFSA)(2,2'\text{-bpy})_4] \cdot TFSA \cdot 8H_2O$ (**1**) and $\{[Cu(4,4'\text{-bpy})(H_2O)_2] \cdot TFSA \cdot 6H_2O\}_n$ (**2**) were presented. The two complexes have extensive hydrogen bonds between lattice water molecules and free anions, leading to the formation of a hybrid water–anion polymeric assembly including water clusters.

This study provides interesting examples of hybrid water clusters, which model supramolecular structures and have potential importance in biochemistry and supramolecular chemistry.

Supplementary material

The crystallographic data of **1** (CCDC 730733) and **2** (CCDC 730735) can be obtained free of charge from CCDC, 12 Union Road, Cambridge, CB2 1EZ, UK; Fax: +44-1223-336033; Email: deposit@ccdc.cam.ac.uk; www: http://www.ccdc.cam.ac.uk/deposit.

Acknowledgments

We thank the Science and Technology Program, Beijing Municipal Education Commission (KM200910028010) and the National Natural Science Foundation of China (21071101).

References

[1] S.L. James. *Chem. Soc. Rev.*, **32**, 276 (2003).
[2] U. Mueller, M. Schubert, F. Teich, H. Puetter, K. Schierle-Arndt, J. Pastré. *J. Mater. Chem.*, **16**, 626 (2006).
[3] D. Maspoch, D. Ruiz-Molina, J. Veciana. *J. Mater. Chem.*, **14**, 2713 (2004).
[4] C.A. Black, J. Sanchez Costa, W.T. Fu, C. Massera, O. Roubeau, S.J. Teat, G. Aromi, P. Gamez, J. Reedijk. *Inorg. Chem.*, **48**, 1062 (2009).
[5] W.G. Lu, C.Y. Su, T.B. Lu, L. Jiang, J.M. Chen. *J. Am. Chem. Soc.*, **128**, 34 (2006).
[6] C.Y. Su, M.D. Smith, A.M. Goforth, H.C. Zur Loye. *Inorg. Chem.*, **43**, 6881 (2004).
[7] A.U. Czaja, N. Trukhan, U. Müller. *Chem. Soc. Rev.*, **38**, 1284 (2009).
[8] C. Janiak. *Dalton Trans.*, 2781 (2003).
[9] C. Aakeröy, N. Champness, C. Janiak. *CrystEngComm.*, **12**, 22 (2010).
[10] M.L. Wei, C. He, W.J. Hua, C.Y. Duan, S.H. Li, Q.J. Meng. *J. Am. Chem. Soc.*, **128**, 13318 (2006).
[11] T.K. Prasad, M.V. Rajasekharan. *Cryst. Growth Des.*, **8**, 1346 (2008).
[12] S. Neogi, G. Savitha, P.K. Bharadwaj. *Inorg. Chem.*, **43**, 3771 (2004).
[13] J.M. Zheng, S.R. Batten, M. Du. *Inorg. Chem.*, **44**, 3371 (2005).
[14] X. Li, H.L. Sun, X.S. Wu, X. Qiu, M. Du. *Inorg. Chem.*, **49**, 1865 (2010).
[15] S.K. Ghosh, J. Ribas, M.S. El Fallah, P.K. Bharadwaj. *Inorg. Chem.*, **44**, 3856 (2005).
[16] Y.F. Deng, Z.H. Zhou. *J. Coord. Chem.*, **12**, 778 (2009).
[17] J.P. Naskar, M.G.B. Drew, A. Hulme, D.A. Tocher, D. Datta. *CrystEngComm.*, **7**, 67 (2005).
[18] Y.Q. Sun, J. Zhang, Z.F. Ju, G.Y. Yang. *Aust. J. Chem.*, **58**, 572 (2005).
[19] C. Janiak, T.G. Scharmann, W. Günther, F. Girgsdies, H. Hemling, W. Hinrichs, D. Lentz. *Chem. Eur. J.*, **1**, 637 (1996).
[20] F. Zhuge, B. Wu, J. Liang, J. Yang, Y. Liu, C. Jia, C. Janiak, N. Tang, X.-J. Yang. *Inorg. Chem.*, **48**, 10249 (2009).
[21] S. Manikumari, V. Shivaiah, S.K. Das. *Inorg. Chem.*, **41**, 6953 (2002).
[22] U. Mukhopadhyay, I. Bernal. *Cryst. Growth Des.*, **5**, 1687 (2005).
[23] S.K. Ghosh, P.K. Bharadwaj. *Inorg. Chem.*, **43**, 6887 (2004).
[24] X.Q. Lu, J.J. Jiang, C.L. Chen, B.S. Kang, C.Y. Su. *Inorg. Chem.*, **44**, 4515 (2005).
[25] S. Balboa, R. Carballo, A. Castineiras, J.M. González-Pérez, J. Niclós-Gutiérrez. *Polyhedron*, **27**, 2921 (2008).
[26] C.Q. Wan, X. Li, C.Y. Wang, X. Qiu. *J. Mol. Struct.*, **930**, 32 (2009).

[27] L.J. Barbour, G.W. Orr, J.L. Atwood. *Chem. Commun.*, **10**, 859 (2000).
[28] Y. Jin, Y.X. Che, S.R. Batten, P.K. Chen, J.M. Zheng. *Eur. J. Inorg. Chem.*, 1925 (2007).
[29] H.D. Xian, H.Q. Li, X. Shi, J.F. Liu, G.L. Zhao. *Inorg. Chem. Commun.*, **12**, 177 (2009).
[30] C.P. Pradeep, S. Supriya, P.S. Zacharias, S.K. Das. *Polyhedron*, **25**, 3588 (2006).
[31] C. Janiak, T.G. Scharmann, S.A. Mason. *J. Am. Chem. Soc.*, **124**, 14010 (2002).
[32] Q.Y. Liu, X. Li. *CrystEngComm.*, **7**, 87 (2005).
[33] C. Janiak, T.G. Scharmann, K.-W. Brzezinka, P. Reich. *Chem. Ber.*, **128**, 323 (1995).
[34] C. Janiak, T.G. Scharmann, H. Helmling, D. Lentz, J. Pickardt. *Chem. Ber.*, **128**, 235 (1995).
[35] C.J. Wang, P.D. Ren, Z.B. Zhang, Y. Fang, Y.Y. Wang. *J. Coord. Chem.*, **62**, 2814 (2009).
[36] X. Li, Y.Q. Li, X.J. Zheng, H.L. Sun. *Inorg. Chem. Commun.*, **11**, 779 (2008).
[37] S. El-Din, H. Etaiw, M.M. El-Bendary. *J. Coord. Chem.*, **63**, 1038 (2010).
[38] J.H. Song, X. Li, Y.Q. Zou. *J. Coord. Chem.*, **63**, 223 (2010).
[39] Y. Jiang, X.S. Wu, X. Li, J.H. Song, Y.Q. Zou. *J. Coord. Chem.*, **63**, 6 (2010).
[40] R. Ludwing. *Angew. Chem. Int. Ed.*, **40**, 1808 (2001).
[41] L. Infantes, S. Motherwell. *CrystEngComm.*, **4**, 454 (2002).
[42] R.R. Fernandes, A.M. Kirillov, M.F.C. Guedes da Silva, Z. Ma, J.A.L. da Silva, J.J.R. Frausto da Silva, A.J.L. Pombeiro. *Cryst. Growth Des.*, **8**, 782 (2008).
[43] W.J. Shi, L. Hou, D. Li, Y.G. Yin. *Inorg. Chim. Acta*, **360**, 588 (2007).
[44] X. Li, Y.B. Zhang, M. Shi, P.Z. Li. *Inorg. Chem. Commun.*, **11**, 869 (2008).
[45] X. Li, Y.B. Zhang, Y.Q. Zou. *J. Mol. Struct.*, **919**, 277 (2009).
[46] J.A. Ibers, W.C. Hamilton. *International Tables for X-ray Crystallography*, Vol. 4, Kynoch Press, Birmingham, UK (1974).
[47] M. Sheldrick. *SHELXL-97*, University of Göttingen, Göttingen, Germany (1997).
[48] D.G. Golovanov, K.A. Lyssenko, M.Yu. Antipin, Y.S. Vygodskii, E.I. Lozinskaya, A.S. Shaplov. *CrystEngComm.*, **7**, 53 (2005).
[49] G. Althoff, J. Ruiz, V. Rodríguez, G. López, J. Pérez, C. Janiak. *CrystEngComm.*, **8**, 662 (2006).
[50] S. Takahashi, T. Jukurogi, T. Katagiri, K. Uneyama. *CrystEngComm.*, **8**, 320 (2006).
[51] A.R. Choudhury, T.N.G. Row. *CrystEngComm.*, **8**, 265 (2006).
[52] R. Mariaca, N.-R. Behrnd, P. Eggli, H. Stoeckli-Evans, J. Hulliger. *CrystEngComm.*, **8**, 222 (2006).
[53] E. D'Oria, J.J. Novoa. *CrystEngComm.*, **10**, 423 (2008).
[54] G.R. Desiraju, T. Steiner. *The Weak Hydrogen Bond*, IUCr Monograph on Crystallography, Vol. 9, Oxford University Press, Oxford (1999).
[55] A.H. Narten, W.E. Thiessen, L. Blum. *Science*, **217**, 1033 (1982).
[56] D. Eisenberg, W. Kauzmann. *The Structure and Properties of Water*, Oxford University Press, New York (1969).
[57] S.W. Jin, W.Z. Chen. *Inorg. Chim. Acta*, **360**, 3756 (2007).